



Evaluation of Dual Electrode Configurations for Microchip Electrophoresis Used for Voltammetric Characterization of Electroactive Species

Journal:	<i>Analyst</i>
Manuscript ID	AN-ART-10-2019-002112.R1
Article Type:	Paper
Date Submitted by the Author:	20-Nov-2019
Complete List of Authors:	Gunasekara, Dulan; University of Kansas, Adams Institute for Bioanalytical Chemistry; University of Kansas, Department of Chemistry Wijesinghe, Manjula; University of Kansas, Adams Institute for Bioanalytical Chemistry; University of Kansas, Department of Chemistry Pichetsurnthorn, Pann; University of Kansas, Adams Institute for Bioanalytical Chemistry; University of Kansas, Department of Chemistry Lunte, Susan; University of Kansas, Adams Institute for Bioanalytical Chemistry; University of Kansas, Department of Chemistry; University of Kansas, Department of Pharmaceutical Chemistry

1
2
3 **Evaluation of Dual Electrode Configurations for Microchip Electrophoresis**
4
5
6 **Used for Voltammetric Characterization of Electroactive Species**
7
8

9 Dulan B. Gunasekara,^{1,2} Manjula B. Wijesinghe,^{1,2} Pann Pichetsurnthorn,^{1,2} Susan M. Lunte^{1,2,3}

11 1. Ralph N. Adams Institute for Bioanalytical Chemistry, University of Kansas, Lawrence, KS,
12 USA.
13

14 2. Department of Chemistry, University of Kansas, Lawrence, KS, USA.
15

16 3. Department of Pharmaceutical Chemistry, University of Kansas, Lawrence, KS USA
17
18
19
20

21 **Correspondence:**

22 Professor Susan M. Lunte

23 Ralph N. Adams Institute for Bioanalytical Chemistry, University of Kansas,
24 2030 Becker Drive, Lawrence, KS 66047, USA

25 E-mail: slunte@ku.edu

26 Phone: +1-785-864-3811

27 Fax: +1-785-864-1916
28
29
30
31
32
33
34
35
36
37
38
39
40
41
42
43
44
45
46
47
48
49
50
51
52
53
54
55
56
57
58
59
60

Abstract

Microchip electrophoresis coupled with amperometric detection is more popular than voltammetric detection due to the lower limits of detection that can be achieved. However, voltammetry provides additional information about the redox properties of the analyte that can be used for peak identification. In this paper, two dual electrode configurations for microchip electrophoresis are described and evaluated for obtaining voltammetric information using amperometry. The dual-series electrode configuration was first evaluated to generate current ratios in a single run by applying two different potentials to the working electrodes placed parallel to the separation channel. However, it was found that it is difficult to obtain realistic current ratios with this configuration, primarily due to the relative placement of electrodes with respect to the channel end of the simple-t microchip. Correction factors were needed to obtain current ratios similar to those that would be obtained for sequential injections at two different potentials using a single electrode. A second approach using a dual-channel chip with two parallel electrodes was then developed and evaluated for obtaining voltammetric identification. The newly developed microchip permitted the injection of same amount of sample into two unique separation channels, each with an electrode at a different detection potential. Migration times and current ratios for several biologically important molecules and potential interferences including nitrite, tyrosine, hydrogen peroxide, and azide were obtained and compared to the responses obtained for analytes found in macrophage cell lysates.

Introduction

Microchip electrophoresis (ME) and capillary electrophoresis (CE) coupled with electrochemical detection (EC) have been used for the separation and detection of many electrochemically active species, including phenolic compounds, reactive nitrogen and oxygen species and their metabolites, inorganic ions, and various other organic molecules.¹⁻⁴ In general, amperometry is favored over voltammetry because lower detection limits can be achieved due to the absence of charging currents. Voltammetric detection using conventional scan rates does not provide adequate temporal resolution for most ME separations.⁵⁻⁷ On the other hand, fast scan voltammetric methods can provide information regarding the half-wave potential of the analyte, which can then be used for peak identification when combined with migration time. There have been several reports of voltammetric detection methods,^{8,9} including fast scan cyclic voltammetry⁷ and square wave voltammetry,¹⁰ for CE. Sinusoidal voltammetry has also been used with ME with high sampling rates.¹¹

Voltammetric information that leads to the identification of a species based on its redox potential cannot be achieved using amperometric detection at a single electrode within a single run. To obtain this information with a single electrode, samples must be analyzed a second time at a different potential. This approach does not work for labile chemical species or with volume-limited samples. To circumvent this problem, dual electrode configurations have been employed in conjunction with separation methods. In the dual-series configuration, two electrodes are placed across the channel perpendicular to the flow, and the sample plug travels sequentially over these electrodes. If one electrode is set at an oxidizing potential and the second at a reducing potential, or vice versa, then compounds undergoing chemically reversible electrochemical reactions can be selectively detected. This configuration has been applied extensively with liquid chromatography

1
2
3 (LC),¹²⁻¹⁴ CE-EC,¹⁵⁻¹⁸ and ME-EC¹⁹⁻²¹ for the selective detection of catecholamines and phenolic
4
5 acids.^{16, 17}
6

7
8 This generation-collection mode can also be used to identify redox active species that
9
10 undergo chemically reversible reactions based on the collection efficiency, which is defined as the
11
12 ratio of current generated from the redox reaction at the second electrode to current produced from
13
14 the original redox reaction at the first electrode. The collection efficiency is dependent on the
15
16 electrochemical rate constant, the distance between the two electrodes, and the flow rate. Species
17
18 having different heterogeneous kinetic rates can therefore be identified based on their collection
19
20 efficiencies, along with their migration times. This configuration has been employed previously
21
22 with microchip electrophoresis to generate current ratios (collection efficiencies) that can be used
23
24 for peak identification.¹⁹ The series electrode arrangement is easily integrated into a simple-t
25
26 microchip; however, the relative placement of the two electrodes and electrolysis of the analytes
27
28 at the first electrode must be optimized to generate good results. In addition, this method has not
29
30 been utilized to generate current ratios to identify redox species separated by ME.
31
32
33
34

35
36 The other electrode arrangement used for voltammetric identification is the dual-parallel
37
38 configuration. This has been used with liquid chromatography²² and CE²³ for compound
39
40 identification. In this mode, the analyte plug travels simultaneously over two working electrodes
41
42 set at two different potentials to generate a current ratio. In contrast to the series electrode
43
44 arrangement, analyte depletion and peak width differences at the two electrodes need not be
45
46 considered.²³ A dual-parallel configuration for ME-EC has not yet been reported.
47
48

49
50 In this paper, both dual-parallel and dual-series electrode configurations are described for
51
52 microchip electrophoresis and evaluated for voltammetric characterization of redox species. The
53
54 development of correction factors to account for differences in current response due to electrode
55
56
57
58
59
60

1
2
3 placement in the dual-series configuration is described. In addition, a dual-channel/dual-electrode
4 microchip that can be used for current ratioing is described. This chip enables injection of the
5 same amount of sample into two unique separation channels, each coupled to a detector electrode.
6
7 This latter configuration is evaluated for the analysis of pro-oxidants and antioxidants present in
8
9
10
11
12
13
14
15
16
17
18
19
20
21
22
23
24
25
26
27
28
29
30
31
32
33
34
35
36
37
38
39
40
41
42
43
44
45
46
47
48
49
50
51
52
53
54
55
56
57
58
59
60

Materials and methods

Materials and reagents

The following chemicals and materials were used as received: SU-8 10 photoresist and SU-8 developer (MicroChem Corp., Newton, MA, USA); AZ 1518 photoresist and 300 MIF developer (Mays Chemical Co., Indianapolis, IN, USA); photolithography film masks (50,000 dpi; Infinite Graphics Inc., Minneapolis, MN, USA); N(100) 100 mm (4") silicon (Si) wafers (Silicon, Inc., Boise, ID, USA); chrome and AZ1518 positive photoresist coated soda lime glass substrates (4" × 4" × 0.090", Nanofilm, Westlake, CA, USA); Sylgard 184 Silicone Elastomer Kit: polydimethylsiloxane (Ellsworth Adhesives, Germantown, WI, USA); titanium (Ti) etchant (TFTN; Transene Co., Danvers, MA, USA); epoxy and 22-gauge Cu wire (Westlake Hardware, Lawrence, KS, USA); silver colloidal paste (Ted Pella, Inc., Redding, CA, USA); acetone, 2-propanol (isopropyl alcohol, IPA), 30% H₂O₂, H₂SO₄, HNO₃, NaOH, and HCl (Fisher Scientific, Fair Lawn, NJ, USA); sodium nitrite, boric acid, tetradecyltrimethylammonium bromide (TTAB), tetradecyltrimethylammonium chloride (TTAC), tyrosine (Tyr), sodium azide, potassium iodide, NaCl, (Sigma, St. Louis, MO, USA); buffered oxide etchant (JT Baker, Austin, TX, USA), and ONOO⁻ (Cayman Chemicals, Ann Arbor, MI, USA or EMD Millipore, Billerica, MA, USA). All water used was ultrapure (18.2 MΩ.cm) (Milli-Q Synthesis A10, Millipore, Burlington, MA, USA).

PDMS device fabrication

The fabrication of PDMS-based microfluidic devices has been described previously.²⁴ Microfluidic channel designs were created using AutoCad LT 2004 (Autodesk, Inc., San Rafael, CA, USA) and printed onto a transparency film at a resolution of 50,000 dpi (Infinite Graphics Inc., Minneapolis, MN, USA). A simple-t device containing a 5-cm separation channel (from the t intersection to the end of the separation channel) and 0.75 cm side arms was used for dual-series configuration (Figure 1A). The first electrode is aligned at the in-channel configuration and the second electrode is aligned at the end-channel electrode.

The design of the dual-channel/dual-electrode (parallel configuration) microchip is shown in Figure 1B. The two separation channels were each 5 cm long. The other dimensions are given in Figure 1B. For both configurations, the width and depth of the electrophoresis microchannels were 40 μm and 14 μm , respectively. All PDMS microstructures were made by casting a 10:1 mixture of PDMS elastomer and curing agent, respectively, against the patterned Si master and curing at 70 °C overnight. Holes for the reservoirs were created in the polymer using a 4 mm biopsy punch (Harris Uni-core, Ted Pella Inc., Redding, CA, USA).

Platinum electrode fabrication

All electrochemical measurements were made using 15 μm Pt working electrodes. Electrodes were fabricated using an in-house magnetron sputtering system (AXXIS DC magnetron sputtering system, Kurt J. Lesker Co., Jefferson Hills, PA, USA). The electrode fabrication protocol was reported earlier by our group.²⁵ For the dual-series electrode configuration, two 15- μm Pt electrodes were placed 15 μm apart (Figure 2A). These designs were created using AutoCad LT 2004 (Autodesk) and printed onto a transparency film at a resolution of 50,000 dpi (Infinite Graphics). The width and height of the resulting Pt electrodes were measured using an Alpha-step

1
2
3 200 profilometer after the electrode preparation (Alpha Step-200, Tencor Instruments, Mountain
4 View, CA, USA).
5
6

7 **Solution preparation**

8
9
10 All solutions were prepared in 18.2 M Ω .cm ultrapure water (Millipore A10 system,
11 Burlington, MA, USA). Stock solutions of nitrite (NaNO₂, 10 mM), hydrogen peroxide (H₂O₂, 10
12 mM), KI (5 mM), and NaN₃ (5 mM) were all prepared in ultrapure water and stored at 4 °C. The
13 tyrosine stock solution was prepared in acidified water (using HCl) to give a final concentration
14 of 10 mM. Subsequent solutions were prepared by diluting the stock solutions in the background
15 electrolyte (BGE) to the appropriate concentration at the time of analysis. Boric acid (50 mM) and
16 TTAB (200 mM) stock solutions were prepared in ultrapure water. The BGE was prepared by
17 first diluting 2 mL of boric acid stock solution in 7 mL of water and followed by adjusting the pH
18 to 11 with 1 M NaOH. Then, 100 μ L of the TTAB stock solution was added and the volume was
19 adjusted to 10 mL with water to give a final borate concentration of 10 mM and 2 mM TTAB.
20
21
22
23
24
25
26
27
28
29
30
31
32

33 **Chip construction and electrophoresis procedure**

34
35 Reversibly sealed PDMS-glass hybrid devices were used for all separations. A Pinnacle
36 isolated potentiostat (Pinnacle Technology Inc., Lawrence, KS, USA), a Ag/AgCl reference
37 electrode (Bioanalytical Systems, West Lafayette, IN, USA), a Pt counter electrode and a 15 μ m
38 Pt working electrode fabricated were used as described above.
39
40
41
42
43

44
45 Electrophoretic separations were performed under reverse polarity mode with TTAB used
46 as the cationic surfactant to produce a stable electroosmotic flow. For the single-channel dual-
47 series experiments, a Pt lead was placed in each reservoir (buffer, sample, buffer waste, sample
48 waste) of a simple-t microchip (Figure 1A). High voltages of -2400 V and -2200 V were applied
49 to the buffer and sample reservoirs, respectively, while the other two reservoirs were grounded
50
51
52
53
54
55
56
57
58
59
60

1
2
3 (Figure 1A). For the dual-channel/dual-electrode (parallel configuration) experiment, sample was
4 placed in reservoir S and all other reservoirs and channels were filled with BGE. A high voltage
5 of -1400 V was applied to the sample reservoir (S) and -2400 V was applied to the buffer
6 reservoirs (B) (Figure 1B). Reservoirs SW and BW were grounded to direct sample into the
7 channels for injection to each channel. An electrokinetic gated injection procedure was applied for
8 each dual-series and dual-parallel experiment with an injection time of 1 s. All of these operations
9 were controlled using home-built LabView software.
10
11
12
13
14
15
16
17
18

19 **Electrochemical detection**

20
21 Three different Pinnacle prototype electrically isolated potentiostats were used for
22 electrochemical detection. These were models 8151P, 8100-K6, and 9051 with sampling rates of
23 5 Hz (gain = 5,000,000 V/A, resolution = 30 fA), 10 Hz (gain = 5,000,000 V/A, resolution = 27
24 fA), and 6.5 to 13 Hz (gain = 5,000,000 V/A, resolution = 47 fA), respectively. The 9051 model
25 was used for the dual series configuration and the other two (8151P and 8100-K6) were employed
26 for the dual-channel dual parallel electrode experiments. Pinnacle Acquisition Laboratory (PAL
27 or Sirenia) software was used for all data acquisition. Data acquisition was performed via wireless
28 data transmission or Bluetooth from the potentiostat to a computer. A working electrode potential
29 of $+1100$ mV or 950 mV vs. Ag/AgCl was used for all experiments.
30
31
32
33
34
35
36
37
38
39
40
41
42
43

44 **Results and discussion**

45 **Theoretical background of generating current ratios for voltammetric identification**

46
47 To obtain a current ratio using ME or CE with amperometric detection and a single working
48 electrode, two separate electropherograms are recorded at two different working electrode
49 potentials. To obtain the best results, one of the selected potentials should be at the current-limiting
50 plateau and the second in the vicinity of the half-wave potential of the analyte of interest. The
51
52
53
54
55
56
57
58
59
60

1
2
3 resultant current ratio can be used for peak verification. Figure 3A shows hypothetical
4 hydrodynamic voltammograms for three analytes with distinct half-wave potentials. For each
5 species, a unique current ratio will be generated if the two potentials indicated in Figure 3B are
6 selected. This current ratio describes the relative ease or difficulty of oxidizing the species. The
7 current ratio of zero obtained at working electrode potentials of +950 mV and +1100 mV for
8 species C in Figure 3B indicates that species C is difficult to oxidize relative to species A and B.
9 Under similar conditions, the current ratio of species A is 1 and, thus, it is the easiest to oxidize.
10 Species B describes a case between species A and C. That is, analytes of interest can be
11 categorized on a zero-to-one comparative scale.
12
13
14
15
16
17
18
19
20
21
22
23

24 This voltammetric information can then be combined with migration time for more
25 conclusive analyte identification. To generate useful current ratios for identification of common
26 intercellular species such as glutathione, ascorbic acid, tyrosine, hydrogen peroxide and nitrite, a
27 potential of +1100 mV vs. Ag/AgCl was chosen as the current-limiting plateau potential. Nitrite
28 does not reach its current-limiting plateau at +1100 mV;²⁶ however, +1100 mV was the maximum
29 potential that could be applied based on the anodic potential window of the BGE.
30
31
32
33
34
35
36
37

38 **Dual-series electrode configuration for ME**

39
40 Determination of the current ratio for an analyte using a single electrode is inconvenient
41 and cannot be applied to short-lived species or volume-limited samples. A dual electrode
42 configuration makes it possible to obtain electropherograms at two different detection potentials
43 in a single run (Figure 2A and B). This can be accomplished in ME with two electrodes either in
44 a dual-series (Figure 1A and Figure 2A) or dual-parallel (Figure 1B and Figure 2B) configuration.
45
46
47
48
49
50

51 For the dual-series electrode configuration, a 5-cm single channel simple-t microchip with
52 two 15- μ m Pt working electrodes with a 15 μ m space between them was employed (Figure 1A).
53
54
55
56
57
58
59
60

1
2
3 However, current ratios obtained using this configuration differed from those obtained using
4 multiple injections using a single electrode; this was due to several factors. In the series
5 configuration, the first electrode “sees” the analyte plug before it reaches the second electrode, and
6 a considerable amount of analyte is lost at the first electrode due to electrolysis. The peaks are also
7 broader at the second electrode due to the end-channel electrode alignment, which can decrease
8 the current response at that electrode. Additionally, when the electrodes are closely placed,
9 overlap of the diffusion layers can occur and lead to reduced mass transport to the second electrode
10 and a lower current response.²⁷ This latter effect can be overcome by increasing the spacing
11 between the two electrodes; however, this will decrease the separation efficiency and resolution of
12 peaks detected at the second electrode. In the discussion of this configuration, the difference in
13 current response observed at the first and the second electrodes, due to the factors indicated above,
14 will be referred to as the “oxidation ratio difference (ORD)”. The ORD can be determined by
15 having both electrodes at the same oxidation potential and measuring the relative current response.
16
17
18
19
20
21
22
23
24
25
26
27
28
29
30
31
32

33 Another drawback of the series configuration for peak identification is that there will be a
34 response difference between two electrodes due to the difference in their positions relative to
35 ground at the channel end. The first electrode is placed with an in-channel configuration (at the
36 exact end of the channel), leaving the second electrode in the end-channel configuration. The
37 response difference between in- and end-channel configurations has been calculated previously to
38 be about a factor of 2.²⁶ Therefore, in the dual-series configuration, the current ratios must be
39 corrected to take these factors into account.
40
41
42
43
44
45
46
47
48

49 To determine the correction factors (ORD and response difference) for the series
50 configuration, standards were first injected and detected with both electrodes set to +1100 mV vs.
51 the Ag/AgCl reference. After three injections, the in-channel electrode was switched off. Three
52
53
54
55
56
57
58
59
60

1
2
3 more injections were then recorded for the end-channel electrode (Figure 4). The response
4
5 difference for each analyte was calculated by taking the ratio of peak currents obtained at the end-
6
7 channel electrode when the in-channel electrode is switched off to the peak current obtained at the
8
9 in-channel electrode. The ORD for each analyte is calculated by subtracting the response
10
11 difference from the current ratio of in-channel and end-channel electrodes when both electrodes
12
13 are on.
14
15

16
17 The results show that the response difference between the in- and end-channel electrodes
18
19 was the most important parameter to be considered (current response ratio in Table 1). The current
20
21 ratios obtained before and after correction for model analytes are shown in the Table 1. For
22
23 example, the current ratio of tyrosine decreased from 2.26 to 1.11 with the response correction (the
24
25 response difference between electrodes is 2.03, Table 1). Tyrosine exhibits a current ratio slightly
26
27 higher than 1 due to the higher response at the in-channel electrode compared to the end-channel
28
29 electrode. However, after the corrections for the response difference were applied, both nitrite and
30
31 hydrogen peroxide showed current ratios less than 1, which obey the theoretical predictions.
32
33

34
35 The error due to the ORD was substantial for easily oxidized species (e.g. tyrosine) but for
36
37 other compounds, it was much lower than the response difference. For example, there was no
38
39 significant difference in the nitrite peak height at the end-channel electrode when the potentiostat
40
41 connected to the in-channel electrode was switched-on vs. when the in-channel electrode was
42
43 switched-off (Figure 4 and ORD in Table 1). This difference can be explained based on the half-
44
45 wave potentials of tyrosine and nitrite ($E_{1/2}$ of tyrosine is 700 mV vs. $E_{1/2}$ of nitrite is 1000 mV)
46
47 under these same conditions (Figure 4 and correction factor for oxidation ratio difference at the
48
49 two electrodes in Table 1). Thus, the impact of ORD is more significant for the easily oxidized
50
51 compounds.
52
53
54
55
56
57
58
59
60

1
2
3 The current ratio value for hydrogen peroxide was 0.91 after the response factor correction.
4
5 This is different than that obtained using ME with a single electrode,²⁶ where a ratio greater than
6
7 1 was observed. It has been shown that the oxidation current for hydrogen peroxide decreases at
8
9 working electrode potentials above +950 mV under the same conditions. The water oxidation at
10
11 the ground electrode that produces oxygen and causes changes in pH may have a different impact
12
13 at the two electrodes, and that may be the reason to observe a different current ratio from a single
14
15 channel experiment. In summary, the dual-series configuration is easier to fabricate than the dual-
16
17 channel dual electrode microchip described below. However substantial corrections need to be
18
19 performed to obtain realistic current ratios for analyte identification, making this approach not very
20
21 convenient for routine analysis.
22
23
24
25

26 **Dual-parallel electrode configurations with ME**

27
28 The use of a dual-parallel configuration was next evaluated for voltammetric identification
29
30 following ME. In this configuration, a microchip with two separation channels was utilized. The
31
32 design was based on one that was first reported by Hahn's group as a noise subtraction method for
33
34 ME-EC (Figure 1B).^{28, 29} In the original report, two electrodes were placed inside two distinct
35
36 channels at the same position relative to the end of the channel. In their experiments, one electrode
37
38 was employed as the working electrode while the second was used as a pseudo reference electrode.
39
40 The BGE was always injected into both channels (from reservoirs P and Q in Figure 1B); however,
41
42 the sample was injected only into the channel containing the working electrode. BGE was injected
43
44 into the channel containing the pseudo-reference electrode in place of sample.
45
46
47
48

49 In Hahn's configuration, two separate reservoirs (Figure 1B, reservoirs Y and Z) were
50
51 utilized for the injection of sample and run buffer. In our studies, a new approach was designed in
52
53 which the sample was placed into a single reservoir (Figure 1B, reservoir X) and it is then divided
54
55
56
57
58
59
60

1
2
3 and injected into two separation channels. The applied voltages were optimized to obtain a proper
4 gating with an injection of equal amounts of samples into two channels under normal polarity with
5 fluorescein (Figure 2D). In these experiments, a background electrolyte consisting of 10 mM boric
6 acid with 2 mM SDS at pH 11 was employed. The sample and separation voltages were +1400 V
7 and +2400 V, respectively. The optimized voltages were then used in the reverse polarity mode
8 for the separation of analytes with the same BGE without SDS.
9
10
11
12
13
14
15

16
17 The ME separations with dual-parallel EC detection experiments were carried out using
18 reverse polarity with TTAB as the channel modifier. The separation buffer consisted of 10 mM
19 boric acid with 2 mM TTAB at pH 11. The sample and buffer voltages were -1400 V and -2400
20 V respectively. The sample injection reproducibility was investigated and reproducible peak
21 heights were obtained for both channels with a RSD less than 6% (Figure 5A and Table 2). These
22 results showed that sample generates similar current responses at the two electrodes following
23 simultaneous injection into the two unique separation channels.
24
25
26
27
28
29
30
31
32

33 In this dual-parallel configuration, both electrodes were placed in the in-channel
34 configuration (Figures 1B and 2B). A similar current response was obtained for each analyte when
35 both electrodes were held at the potential of +1100 mV (Figure 5A and Table 2). In addition, the
36 current response for all tested analytes (nitrite, azide, iodide, and tyrosine) except hydrogen
37 peroxide decreased when the potential at one of electrodes was lowered from +1100 to +950 mV
38 vs. Ag/AgCl (Figure 5B). Therefore, current ratios for each analyte could be calculated using this
39 dual-electrode/dual-channel configuration without performing any corrections, as shown in Table
40
41
42
43
44
45
46
47
48
49 2.
50

51 It was also noted that a response difference between the two working electrodes was
52 observed in some experiments with the dual-parallel electrode configuration. This was due to
53
54
55
56
57
58
59
60

1
2
3 variability in the microfabrication process and precise placement of the electrodes. When this
4 occurred, the response difference could be easily corrected by applying the same potential to both
5 electrodes and normalizing the response. In these studies, the surface area of the electrodes exposed
6 to the solution was assumed to be the same. However, if electrode areas are different, this could
7 lead to changes in peak current and affect the current ratio. To assure that the ratios were accurate,
8 the dual-parallel configuration current responses were determined using standards before running
9 any biological samples. However, in general, our results show that the dual-parallel configuration
10 allows generation of current ratios without extensive corrections.
11
12
13
14
15
16
17
18
19
20

21 **Use of dual-parallel configuration for improved identification of intracellular electroactive** 22 **species in macrophage cell lysates** 23 24 25

26 Azide from the filter shows up in our cell lysis experiments as an impurity, making it
27 difficult to detect nitrite in these samples.³⁰ As can be seen in Table 2, the migration times of
28 nitrite and azide are very similar; therefore, it is difficult to conclusively identify them by migration
29 time only. Voltammetric characterization can aid in peak identification in this case. As shown in
30 Table 2, the current ratio (I_{950}/I_{1100}) for nitrite is higher than that for azide because it is easier to
31 oxidize. As there was a considerable difference in the response at the two electrodes for azide
32 when compared to other species (Table 2), a correction was made using the I_{1100}/I_{1100} ratio for
33 nitrite and azide for comparison, resulting in current ratios of 0.20 ± 0.02 for nitrite and $0.16 \pm$
34 0.02 for azide, which are statistically different at 95% confidence limit ($n = 3$). Therefore, these
35 current ratios can be applied to distinguish azide from nitrite.
36
37
38
39
40
41
42
43
44
45
46
47
48

49 Identification of electroactive species present in macrophage cell lysates was performed
50 using a dual-channel/dual-parallel microchip. Previously, pseudo-in-channel amperometric
51 detection coupled to a simple-t microchip was employed to identify nitrite, tyrosine, glutathione,
52
53
54
55
56
57
58
59
60

1
2
3 and NO from macrophage cell lysates based on their migration times. In this procedure, the
4 background electrolyte is used to lyse the macrophage cells, followed by filtering through a 3 kDa
5 cut-off filter, before microchip analysis. As we have seen in our previous studies, several redox
6 species appeared in the electropherograms generated for the cell lysate using the dual-parallel/dual
7 channel microchip system. Iodide (species c) was used as an internal standard for the
8 determination of reproducibility of the analyte injection into the two channels and correct operation
9 of the separation and detection system. The electropherograms obtained are shown in Figures 6A
10 and B.
11
12
13
14
15
16
17
18
19
20

21 The current ratios and migration times were calculated for the first four species (Table 3).
22 Peak c was identified as iodide because its migration time and current ratio is close to the value
23 obtained with the standard. The current ratios of the first two peaks in the electropherogram are
24 not statistically different; however, when combined with migration times, it can be concluded that
25 peak a is nitrite and peak b is azide. To further confirm that peak a is nitrite, the sample was spiked
26 with authentic nitrite. The results obtained are shown in Table 3. The peak current ratio for peak a
27 in the cell lysis sample was 0.28 ± 0.08 , which is not statistically different from the nitrite standard
28 (0.20 ± 0.05). When the sample was spiked with nitrite, the height of peak a increased and the
29 current ratio was still in the range of the nitrate standard (0.17 ± 0.05). Although peak d was
30 initially tentatively identified as tyrosine, based on migration time, the peak current ratio obtained
31 for this peak (1.26 ± 0.02) was very different from that of tyrosine (0.77 ± 0.04). Therefore, peak
32 d must be another (easily) oxidizable compound present in the sample. Future studies will attempt
33 to identify this and other compounds in cell lysate samples.
34
35
36
37
38
39
40
41
42
43
44
45
46
47
48
49
50
51
52
53
54
55
56
57
58
59
60

2.4 Conclusions:

It has been shown here that the dual-series electrode configuration for identification of analytes based on current ratios requires time-consuming and comprehensive data analysis, and is therefore not the optimal approach for voltammetric characterization. A better method to collect voltammetric information to identify electroactive species using a dual-parallel configuration is presented. This configuration makes it possible to obtain a current ratio from a single sample in one run, eliminating sample-to-sample variability and making it possible to obtain voltammetric information for short-lived species or volume-limited samples using ME. However, fabrication and electrode alignment require significant attention and care to obtain good results with this approach. The dual channel/dual electrode configuration was used to identify species in macrophage cells based on migration time and voltammetric properties.

Acknowledgements: The authors of this paper would like to acknowledge the National Science Foundation (CHE-1411993) and National Institutes of Health (COBRE P20GM103638). The editorial support provided by Nancy Harmony is gratefully acknowledged. Also, the authors would like to thank Pinnacle Technology, Inc. for the development and supply of prototype potentiostats. Portions of this work were presented in microTAS, Proceedings of the 15th International Conference on Miniaturized Systems for Chemistry and Life Sciences, Washington, DC, 2011.

References

1. N. A. Lacher, K. E. Garrison, R. S. Martin and S. M. Lunte, *Electrophoresis*, 2001, **22**, 2526-2536.
2. A. Martin, D. Vilela and A. Escarpa, *Electrophoresis*, 2012, **33**, 2212-2227.
3. G. Chen, Y. Lin and J. Wang, *Current Analytical Chemistry*, 2006, **2**, 43-50.
4. W. R. Vandaveer IV, S. A. Pasas-Farmer, D. J. Fischer, C. N. Frankenfeld and S. M. Lunte, *Electrophoresis*, 2004, **25**, 3528-3549.
5. S. S. Ferris, G. Lou and A. G. Ewing, *J. Microcolumn Sep.*, 1994, **6**, 263-268.
6. F. D. Swanek, G. Chen and A. G. Ewing, *Anal. Chem.*, 1996, **68**, 3912-3916.
7. H. Fang, T. L. Vickrey and B. J. Venton, *Anal. Chem.*, 2011, **83**, 2258-2264.
8. S. Park, M. J. McGrath, M. R. Smyth, D. Diamond and C. E. Lunte, *Anal. Chem.*, 1997, **69**, 2994-3001.
9. J. Wen, A. Baranski and R. Cassidy, *Anal. Chem.*, 1998, **70**, 2504-2509.
10. G. C. Gerhardt, R. M. Cassidy and A. S. Baranski, *Anal. Chem.*, 1998, **70**, 2167-2173.
11. N. E. Hebert, W. G. Kuhr and S. A. Brazill, *Electrophoresis*, 2002, **23**, 3750-3759.
12. C. E. Lunte, T. H. Ridgway and W. R. Heineman, *Anal. Chem.*, 1987, **59**, 761-766.
13. C. E. Lunte, P. T. Kissinger and R. E. Shoup, *Anal. Chem.*, 1985, **57**, 1541-1546.
14. D. A. Roston, R. E. Shoup and P. T. Kissinger, *Anal. Chem.*, 1982, **54**, 1417A-1434A.
15. M. Zhong, J. Zhou, S. M. Lunte, G. Zhao, D. M. Giolando and J. R. Kirchhoff, *Anal. Chem.*, 1996, **68**, 203-207.
16. M. Zhong and S. M. Lunte, *Anal. Chem.*, 1999, **71**, 251-255.
17. B. L. Lin, L. A. Colón and R. N. Zare, *J. Chromatogr. A*, 1994, **680**, 263-270.
18. L. A. Holland, N. M. Harmony and S. M. Lunte, *Electroanalysis*, 1999, **11**, 327-330.
19. R. S. Martin, A. J. Gawron, S. M. Lunte and C. S. Henry, *Anal. Chem.*, 2000, **72**, 3196-3202.
20. L. C. Mecker and R. S. Martin, *Electrophoresis*, 2006, **27**, 5032-5042.
21. D. J. Fischer, W. R. Vandaveer IV, R. J. Grigsby and S. M. Lunte, *Electroanalysis*, 2005, **17**, 1153-1159.
22. C. E. Lunte and P. T. Kissinger, *Anal. Chem.*, 1983, **55**, 1458-1462.
23. M. K. Dorris, E. W. Crick and C. E. Lunte, *Electrophoresis*, 2012, **33**, 2725-2732.
24. M. K. Hulvey, C. N. Frankenfeld and S. M. Lunte, *Anal. Chem.*, 2010, **82**, 1608-1611.
25. D. E. Scott, R. J. Grigsby and S. M. Lunte, *Chemphyschem*, 2013, **14**, 2288-2294.
26. D. B. Gunasekara, M. K. Hulvey and S. M. Lunte, *Electrophoresis*, 2011, **32**, 832-837.
27. S. Amemiya, A. J. Bard, F.-R. F. Fan, M. V. Mirkin and P. R. Unwin, *Annu Rev Anal Chem*, 2008, **1**, 95-131.
28. C. Chen and J. H. Hahn, *Anal. Chem.*, 2007, **79**, 7182-7186.
29. C. Chen, W. Teng and J. H. Hahn, *Electrophoresis*, 2011, **32**, 838-843.
30. D. B. Gunasekara, J. M. Siegel, G. Caruso, M. K. Hulvey and S. M. Lunte, *Analyst*, 2014, **139**, 3265-3273.

Figure-01

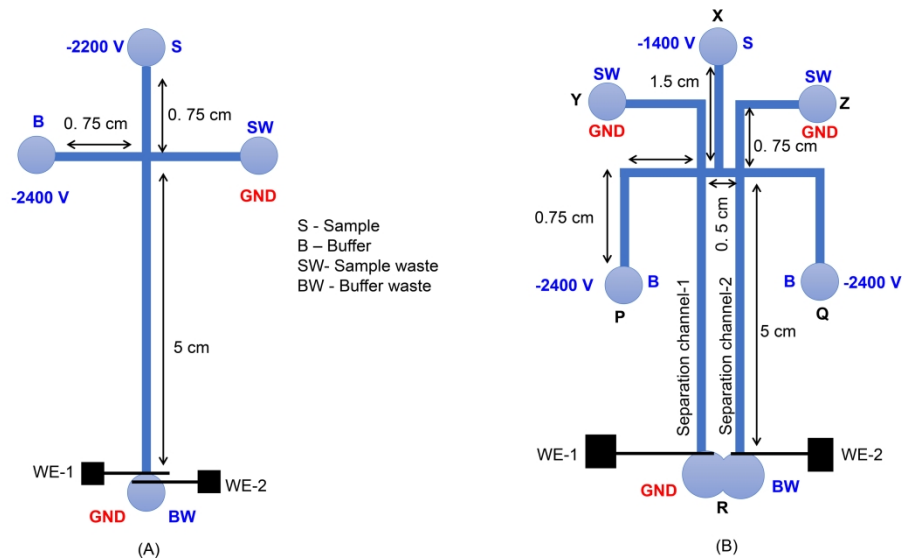


Figure 1. A. Simple-t microchip with dual-series electrodes and placement of sample (S), buffer (B), sample waste (SW), buffer waste (BW) and applied voltages; -2200 V (sample) and -2400 V (buffer). B. Dual-channel microchip design used for dual-parallel electrode configuration (adapted from ref. 29). Width and depth of the electrophoresis microchannels $40\text{ }\mu\text{m}$ and $14\text{ }\mu\text{m}$, respectively. Applied voltages -1400 V (sample) and -2400 V (buffer).

338x190mm (300 x 300 DPI)

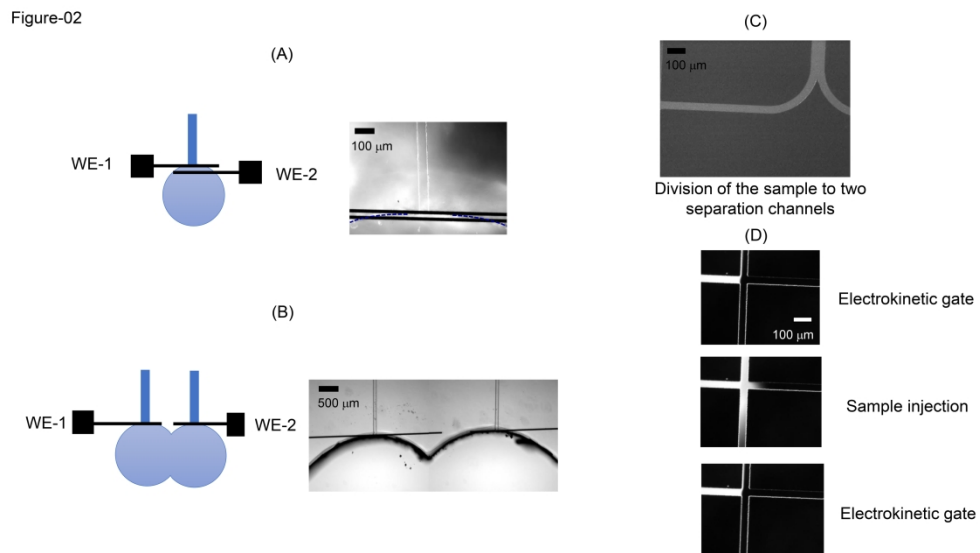


Figure 2. Electrode alignment for A. dual-series configuration and B. dual-parallel configuration; C. filling of equal amounts of sample into the two unique separation channels; D. electrokinetic gated injection of sample into two channels.

338x190mm (300 x 300 DPI)

Figure-03

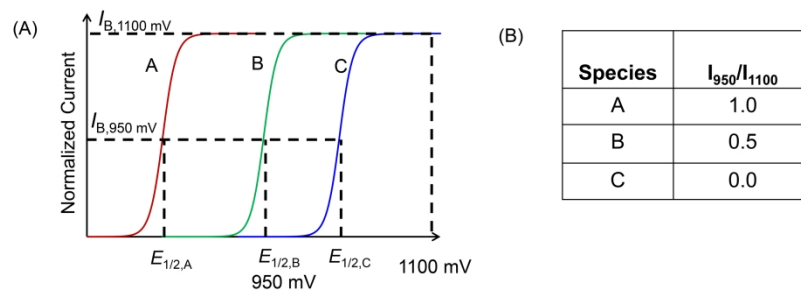


Figure 3. The basis of generation of current ratios by hydrodynamic voltammetry and dual-electrode configurations A. Hypothetical hydrodynamic voltammograms for three species with different $E_{1/2}$; B. list of current ratios generated for each of the species at 950 mV and 1100 mV.

338x190mm (300 x 300 DPI)

Figure-04

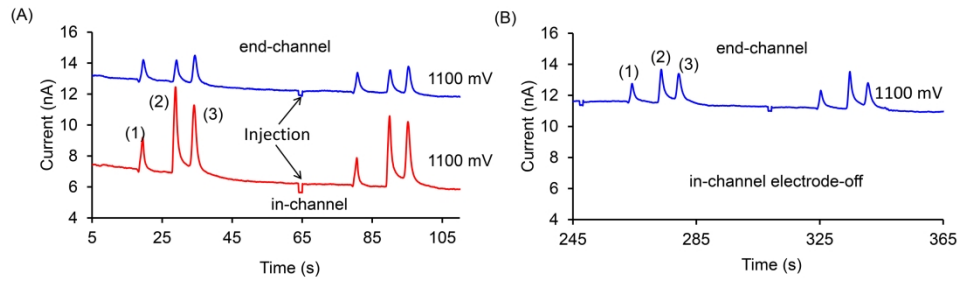


Figure 4. Determination of current ratios for dual-series configuration using (1) nitrite, (2) tyrosine, and (3) H₂O₂ standards. The sample was prepared in 10 mM borate and 2 mM TTAB BGE at pH 11; the separation was achieved using the same buffer. Electropherograms obtained for end-channel and in-channel electrodes at 1100 mV. A. Both electrodes are "switched on." B. In-channel electrode is "switched off."

338x190mm (300 x 300 DPI)

Figure-05

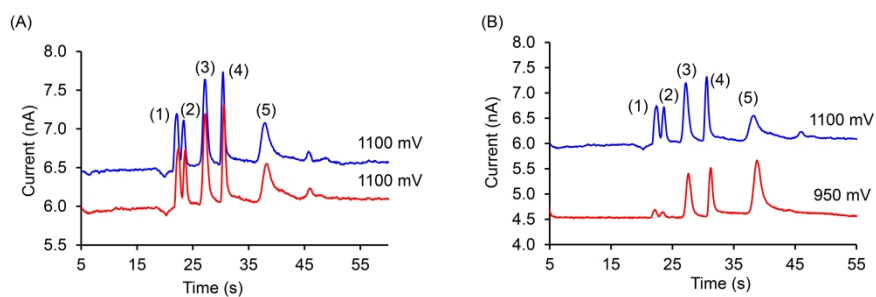


Figure 5. Characterization of dual-channel dual-parallel configuration with (1) nitrite, (2) azide, (3) iodide, (4) tyrosine, and (5) H_2O_2 standards using reverse polarity. The sample was prepared in 10 mM borate and 2 mM TTAB BGE at pH 11; sampling and separation voltages were -1400 V and -2400 V , respectively. (A) WE-1 = WE-2 = $+1100\text{ mV}$ and (B) WE-1 = $+1100$ and WE-2 = $+950\text{ mV}$ vs. Ag/AgCl reference electrode were used.

338x190mm (300 x 300 DPI)

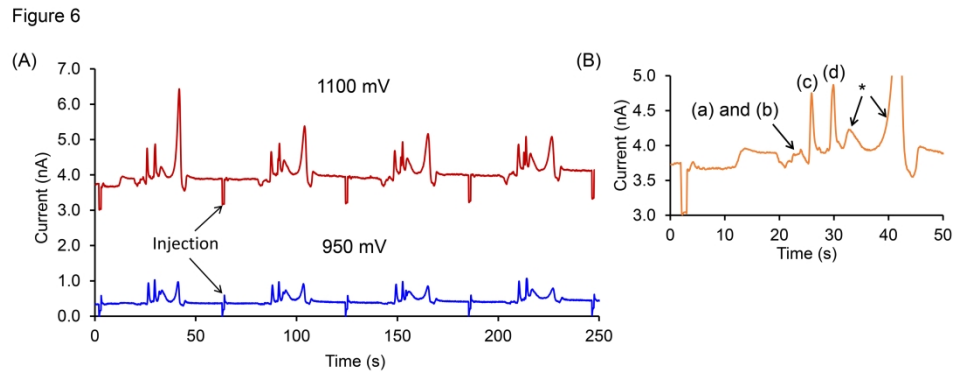


Figure 6. Electropherograms obtained for macrophage cell lysates using dual-parallel electrode configuration. The sample was prepared in 10 mM borate and 2 mM TTAB BGE at pH 11; sampling and separation voltages were -1400 V and -2400 V, respectively. (A) Electropherogram obtained at 1100 mV and 950 mV. (B) Inset showing the tentative peak assignments. *- unidentifiable peaks

338x190mm (300 x 300 DPI)

1
2
3 Table-01
4
5

Species	I_{950}/I_{1100}	Correction factor ORD	Correction factor electrode response ratio	Corrected values with response factor I_{950}/I_{1100}
(1) Nitrite	0.25 ± 0.02	-0.16 ± 0.03	1.65 ± 0.17	0.15 ± 0.02
(2) Tyrosine	2.26 ± 0.02	1.33 ± 0.12	2.03 ± 0.57	1.11 ± 0.31
(3) H ₂ O ₂	2.33 ± 0.12	-0.04 ± 0.26	2.57 ± 0.16	0.91 ± 0.07

6
7
8
9
10
11
12
13
14
15
16
17
18
19
20
21
22
23
24
25
26
27
28
29
30
31
32
33
34
35
36
37
38
39
40
41

1
2
3
4
5
6
7
8
9
10
11
12
13
14
15
16
17
18
19
20
21
22
23
24
25
26
27
28
29
30
31
32
33
34
35
36
37
38
39
40
41

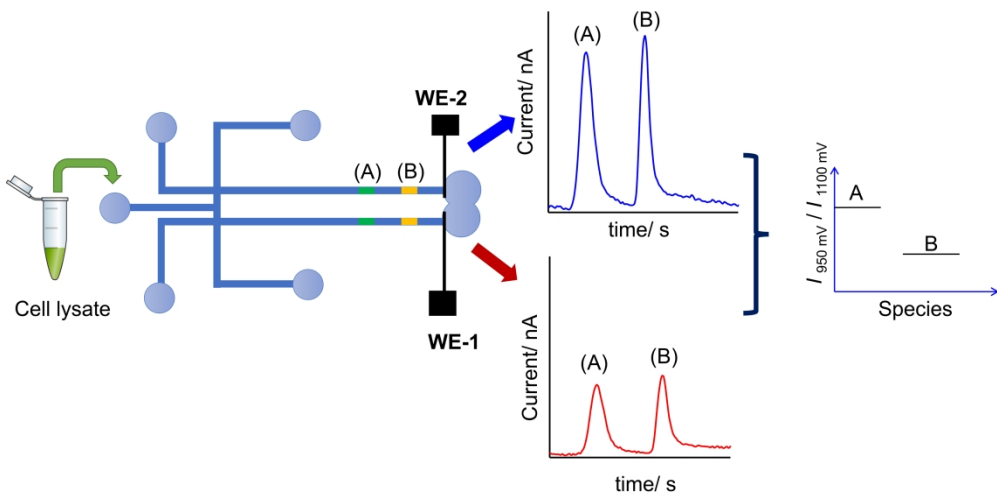
Table-02

Species	Migration time (s)	I_{1100}/I_{1100}	I_{950}/I_{1100}
Nitrite	17.4 ± 0.2	1.04 ± 0.06	0.20 ± 0.02
Azide	18.7 ± 0.2	0.87 ± 0.05	0.16 ± 0.02
Iodide	23.0 ± 0.1	0.98 ± 0.03	0.75 ± 0.02
Tyrosine	26.6 ± 0.0	0.92 ± 0.04	0.77 ± 0.04
H ₂ O ₂	34.4 ± 0.3	1.04 ± 0.06	2.04 ± 0.09

Table-03

Species	Standards		Cells			Cells after spike with Nitrite	
	Migration time (s)	I_{950}/I_{1100}	Tentative Identity	Migration time (s)	I_{950}/I_{1100}	Migration time (s)	I_{950}/I_{1100}
Nitrite	17.4 ± 0.2	0.20 ± 0.02	a	19.6 ± 0.2	0.28 ± 0.08	18.6 ± 0.4	0.17 ± 0.05
Azide	18.7 ± 0.2	0.16 ± 0.02	b	21.6 ± 0.2	0.25 ± 0.08	NA	NA
Iodide	23.0 ± 0.1	0.75 ± 0.02	c	23.6 ± 0.3	0.64 ± 0.08	23.6 ± 0.7	0.63 ± 0.05
Tyrosine	26.6 ± 0.0	0.77 ± 0.04	d	26.5 ± 0.2	1.26 ± 0.02	NA	NA

1
2
3
4
5
6
7
8
9
10
11
12
13
14
15
16
17
18
19
20
21
22
23
24
25
26
27
28
29
30
31
32
33
34
35
36
37
38
39
40
41
42
43
44
45
46
47
48
49
50
51
52
53
54
55
56
57
58
59
60



338x190mm (300 x 300 DPI)